ELSEVIER

Thin Solid Films 408 (2002) 316–320

thin solid films

www.elsevier.com/locate/tsf

# Crystallization behavior of r.f.-sputtered near stoichiometric $Ni_2MnGa$ thin films

S.K. Wu[a,*], K.H. Tseng[b], J.Y. Wang[c]

[a]*Department of Materials Science and Engineering, National Taiwan University, TaipeiTaiwan 106*
[b]*Department of Mechanical Engineering, National Taiwan University, TaipeiTaiwan 106*
[c]*Materials & Electro-Optics Research Division, Chung-Shan Institute of Science and Technology, Lung-TanTaiwan 325*

Received 2 September 2001; accepted 24 January 2002

**Abstract**

Thin films of $Ni_{51.45}Mn_{25.30}Ga_{23.25}$ alloy were deposited onto a 3-inch diameter n-type Si(100) wafer by r.f. magnetron sputtering. The observation of high resolution transmission electron microscopy shows that the as-deposited thin films were partially crystalline and dense, with a preferred growth of $L2_1$ structure nanoparticles. The crystallization activation energy $Q$ of the as-deposited free-standing thin film was found to be 234 kJ/mol by Kissinger's method. The onset crystallization temperature, $T_x$, was 427 °C at the 10 °C/min heating rate. Both $Q$ and $T_x$ are much lower than those of near-equiatomic TiNi alloy mainly due to its inherently partial crystallization in as-deposited films. 

*Keywords:* Near stoichiometric Ni2MnGa alloy; Sputtering; Crystallization; Transmission electron microscopy; Annealing

## 1. Introduction

The near stoichiometric $Ni_2MnGa$ alloys are known as the ferromagnetic shape memory alloys (SMAs) [1–4]. Bulk single crystals of near stoichiometric $Ni_2MnGa$ alloys have shown exceptionally large magnetostriction and thin films of these alloys have been regarded as promising candidates for microelectromechanical systems (MEMS) applications [5,6]. However, the crystallization behavior of $Ni_2MnGa$ thin films have not yet been reported. Dong et al. have grown 300 Å single crystal (001)$Ni_2MnGa$ films on (001)GaAs by the molecular beam epitaxy method [7]. Wuttig and Craciunesco indicate that near stoichiometric $Ni_2MnGa$ films with a thickness of 1 μm can be DC magnetron sputter-deposited on oxidized Si(100) substrates [8]. They found that the as-deposited $Ni_2MnGa$ films, by keeping the substrate temperature at room temperature, were partially crystalline as evidenced by the width of the X-ray diffraction (XRD) $(220)_A$ peak (Subscript A means the parent $L2_1$ phase of $Ni_2MnGa$ alloy). According to the results of near-equiatomic TiNi alloys which are another class of important SMAs, as-sputtered TiNi films onto a non-artificial heated substrate are amorphous and do not behave as SMAs. Therefore, the crystallization behavior, such as the crystallization temperature and its activation energy, is important for the fabrication process of TiNi thin films [9]. We suggest that the understanding of crystallization behavior is also important to thin films of near stoichiometric $Ni_2MnGa$ SMAs as-sputtered at room temperature substrates.

In the present research, $Ni_2MnGa$ thin films with near stoichiometric composition were studied by r.f.-sputtering. Thin films with thicknesses of 1.5 μm and 5 μm were removed from the Si(100) substrate and tested by differential scanning calorimetry (DSC). From DSC data, the crystallization temperature can be determined, and thereafter the activation energy of crystallization can be calculated by Kissinger's method [10]. The microstructure of the peel-off thin film with 5 μm thickness was also observed by a high-resolution transmission electron microscopy (HRTEM). X-Ray diffraction (XRD) tests were also conducted to identify the phases of as-deposited thin films.

*Corresponding author. Tel.: +886-2-2363-7846; fax: +886-2-2363-4562.
*E-mail address:* skw@ccms.ntu.edu.tw (S.K. Wu).

0040-6090/02/$ - see front matter 
PII: S0040-6090(02)00134-7

## 2. Experimental procedure

Near stoichiometric $Ni_2MnGa$ thin films were deposited onto a 3-inch diameter n-type Si(100) wafer in a 2-inch r.f. magnetron sputtering apparatus using a $Ni_2MnGa$ target. The target was prepared by vacuum arc melting from the raw materials of nickel (purity 99.9 wt.%), Mn55–Ni45 mother alloy (in wt.%) and gallium (purity 99.99 wt.%), then homogenized at 850 °C for 48 h, and finally wire-cut into a 2-inch-diameter target disk. The composition of target disk was determined by the electron probe microanalyzer (EPMA) of a JEOL JAX-8600SX instrument and was found to be $Ni_{50.22}Mn_{24.77}Ga_{25.01}$ (in at.%). The sputtering conditions used in this study are given in Table 1. Table 1 also lists the composition of as-sputtered thin films determined by EPMA. This composition was found to be $Ni_{51.45}Mn_{25.30}Ga_{23.25}$ (in at.%).

The sputtered films were peeled from the substrate and then cut into smaller pieces and encapsulated in an aluminum pan for the DSC test. DSC measurement was conducted by a DuPont 2000 thermal analyzer equipped with a quantitative scanning system 910 DSC cell for controlled heating and cooling in pure Ar gas. According to Kissinger's method, data of different heating rates in the DSC test are required for calculating the activation energy of crystallization, in which each heating rate corresponds to its crystallization peak temperature. Thus, samples were put directly into the 300 °C DSC cell and then heated with heating rates of 10, 20, 30, 40 and 50 °C/min to the maximum temperature 580 °C. The amorphous structure and crystallization phases of thin films before and after annealing were confirmed by a Philips PW1719 XRD instrument. Here, XRD tests were conducted by film-on-substrate specimens for as-deposited thin films. The microstructure of peeled-off thin film with 5 μm thickness were also observed by HRTEM. TEM specimens were fabricated by grinding, dimpling and then ion-milling at 5 kV to perforation. Microstructural observation was performed using a HRTEM model JEOL 4000FX operated at 400 kV with 2.6 Å point-to-point resolution and 1.8 Å line-to-line resolution. The ?$L$ value used in this study is 20.6 Å mm with $L$=camera length and ?=0.00031 Å at 400 kV.

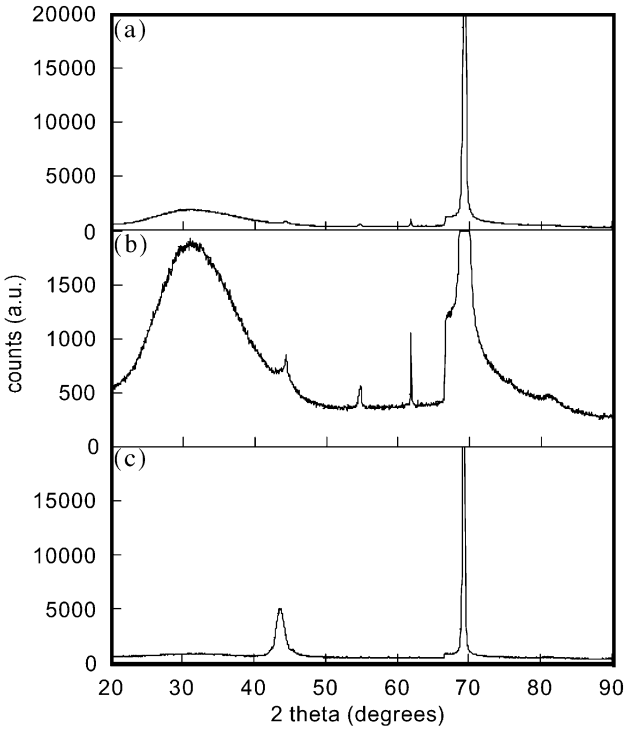


Fig. 1. The XRD tests of as-deposited $Ni_{51.45}Mn_{25.30}Ga_{23.25}$ thin film. (a) The 1.5-μm-thick thin film, (b) the magnified diagram of (a) in the 2? range of 20° to 60°, (c) the 5-μm-thick thin film.

## 3. Results and discussion

### *3.1. XRD and HRTEM tests for the as-deposited thin films*

Fig. 1a shows the XRD spectrum of as-deposited $Ni_{51.45}Mn_{25.30}Ga_{23.25}$ thin film with 1.5 μm thickness, whereas Fig. 1b is the magnified diagram of Fig. 1a in the 2? ranging from 20° to 60°. From Fig. 1a,b, the as-deposited thin film is partially crystallized with $(220)_A$ and $(222)_A$ XRD diffraction peaks appearing at approximately 44° and 55°, respectively, and an amorphous mound appearing at approximately 30°. Fig. 1c is similar to Fig. 2a but now the thin film thickness is 5 μm. From Fig. 1c, the intensities of the amorphous mound and $(222)_A$ peak are both reduced significantly, however, the intensity of $(220)_A$ peak increased remarkably. The

Table 1
Sputtering conditions used in this study and the composition of the sputtered films

| Argon gas pressure (torr) | r.f. power (W) | Sputtered film thickness (μm) | Distance between target and substrate (mm) | Sputtering time (min) | [3]Average composition (at.%) | | |
|---|---|---|---|---|---|---|---|
| | | | | | Ni | Mn | Ga |
| 0.005 | 100 | 1.5–5 | 80 | 90–300 | 51.45 | 25.30 | 23.25 |

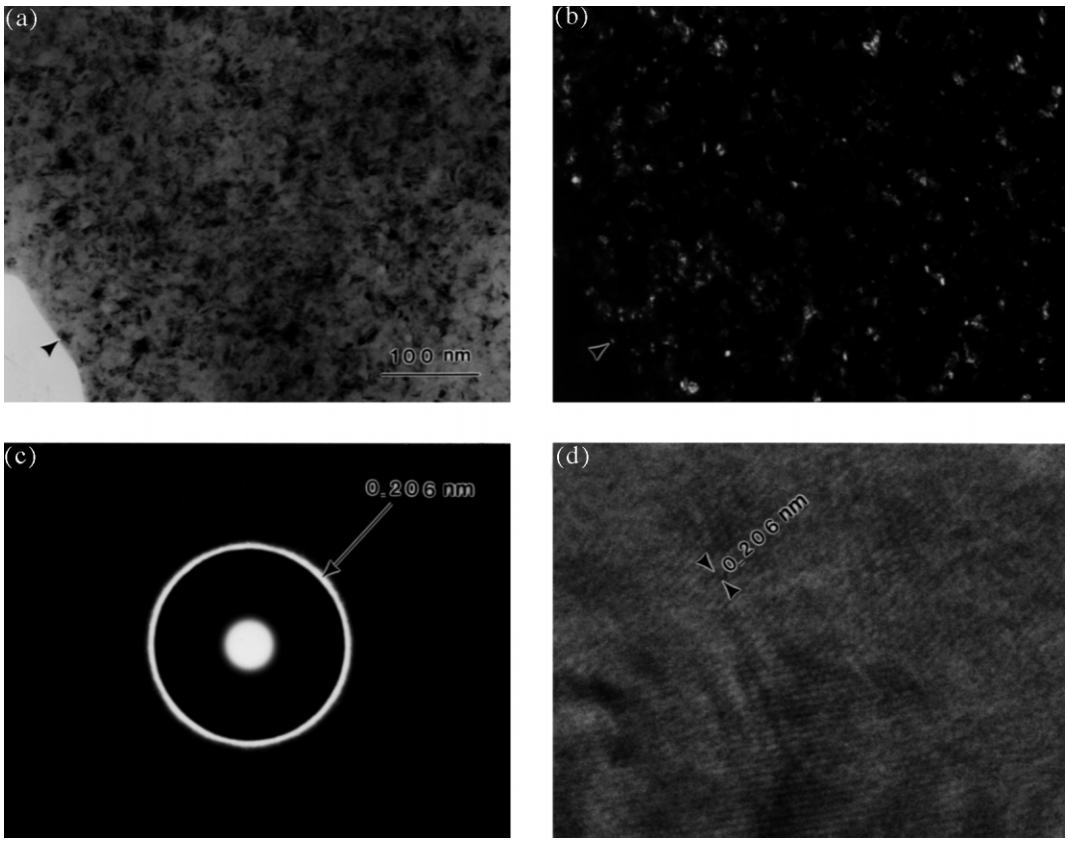


Fig. 2. The HRTEM observation of as-deposited $Ni_{51.45}Mn_{25.30}Ga_{23.25}$ thin film of 5 μm thickness. (a) The bright-field image, (b) the dark-field image, (c) the SADP of (a), (d) the lattice image of crystalline particles of (a).

broadened $(220)_A$ peak and 30° amorphous mound show that the thin film of Fig. 1c is partially crystalline. The HRTEM observation of the specimen of Fig. 1c is shown in Fig. 2, in which Fig. 2a is a bright field image, Fig. 2b is a dark field image. Fig. 2c is a selected area diffraction pattern (SADP) of Fig. 2a and Fig. 2d is the lattice image of Fig. 2a. From Fig. 2, it is further confirmed that the thin film of Fig. 1c is partially crystalline with the ring pattern of the strongest intensity coming from $(220)_A$ planes. Fig. 2d also indicates that the lattice image of crystalline phase corresponds to the distance of $(220)_A$ planes, i.e. 2.06 Å. The crystalline particles in the partially crystalline film are nanoparticles. They are dense and random-distributed with the particles' size being less than 50 nm.

Experimental results of Figs. 1 and 2 also indicate that the as-deposited thin film of $Ni_{51.45}Mn_{25.30}Ga_{23.25}$ alloy has the $(220)_A$ preferred growth in the crystalline phase. Compared with the $(220)_A$ peak intensities of Fig. 1a,c, the $(220)_A$ peak intensity increases with the increase of film thickness. This characteristic comes from the fact that the temperature of substrate increases continuously during the course of sputtering. The higher the substrate temperature, the more the crystalline volume in the as-deposited thin film can be obtained. The ring pattern of the strongest intensity of Fig. 2c is diffracted from the $(220)_A$ planes of $L2_1$ phase and shows a band-type ring, instead of a line-type ring. This phenomenon implies that the plane distance of $(220)_A$ may have a little variation among nanoparticles, as these nanoparticles may have different state of stress in the as-deposited thin film.

### *3.2. Crystallization temperature of sputtered $Ni_{51.45}Mn_{25.30}Ga_{23.25}$ thin films*

Fig. 3a shows a sample heated in a DSC cell with a heating rate 10 °C/min from 300 to 580 °C and crystallized with a single heat peak. After the first heating run, this sample was cooled in the DSC cell to room temperature, and then heated again in the same cell to 580 °C. Fig. 3b shows the DSC result of the second heating run and no heat peak can be detected. The crystallization temperature, taken as the temperature at onset, is 427 °C. This temperature is also indicated as $T_x$ in Fig. 4 in the DSC curve of 10 °C/min heating rate. Wuttig et al.[8] indicate that the film-on-Si substrate of $Ni_{50}Mn_{30}Ga_{20}$ sputtering film annealed at 400 °C can develop the martensitic transformation, i.e. its crystallization temperature is approximately 400 °C. The

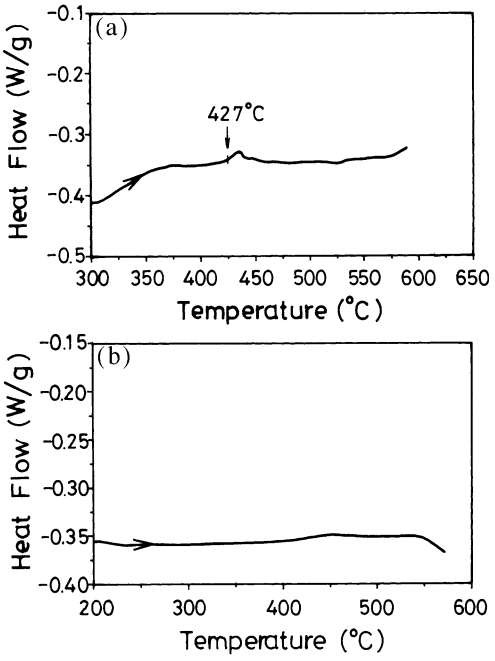


Fig. 3. The DSC curves of as-deposited $Ni_{51.45}Mn_{25.30}Ga_{23.25}$ thin film (5 μm thickness) at the heating rate 10 °C/min. (a) The first heating run from 300 to 580 °C, (b) the second heating run from room temperature to 580 °C (only 200–580 °C is shown in this figure).

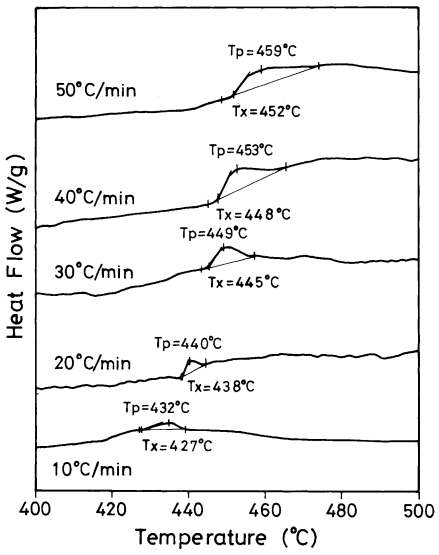


Fig. 4. DSC curves with different heating rates from 300 to 580 °C for the as-deposited $Ni_{51.45}Mn_{25.30}Ga_{23.25}$ thin film (5 μm thickness). The peak temperature $T_p$ and the onset crystallization temperature $T_x$ for each curve are also indicated.

difference of the crystallization temperature of near stoichiometric $Ni_2MnGa$ thin films found in this study and that in Wuttig and Craciunesco [8] may come from the difference of the films' composition and their inherent stress state.

### *3.3. Activation energy of crystallization calculated by Kissinger's method*

The crystallization activation energy of as-deposited thin films with 5 μm thickness can be calculated by Kissinger's method according to the following equation:

$$\ln(\alpha/T_p^2) = C - Q/RT_p \quad (1)$$

where α is the heating rate, $T_p$ is the peak temperature of the DSC curve, $C$ is a constant, $R$ is the gas constant and $Q$ is the crystallization activation energy.

Fig. 4 shows the DSC curves of specimens indicating the peak temperature and the corresponding heating rates. From the data of Fig. 4, $\ln(\alpha/T_p^2)$ vs. $1/T_p$ is plotted in Fig. 5 and the activation energy $Q$ is determined to be 234 kJ/mol. In Fig. 4, the onset crystallization temperature, $T_x$, for each heating rate is also indicated.

The crystallization temperature $T_x$ and crystallization activation energy $Q$ of near-equiatomic TiNi SMAs are much higher than those of near stoichiometric $Ni_2MnGa$ SMAs, say 416 kJ/mol and 511 °C, respectively, for $Ti_{49.93}Ni_{50.07}$ alloy [11], and 234 kJ/mol and 427 °C, respectively, for $Ni_{51.45}Mn_{25.30}Ga_{23.25}$ alloy. We suggest that the as-deposited $Ni_{51.45}Mn_{25.30}Ga_{23.25}$ thin film having partially crystalline, instead of fully amorphous, accounts for the reason why it has much lower $T_x$ and $Q$ values.

## 4. Conclusion

Thin films of $Ni_{51.45}Mn_{25.30}Ga_{23.25}$ alloy were deposited onto a 3-inch diameter n-type Si(100) wafer by r.f. magnetron sputtering without heating the substrate. XRD and HRTEM tests show that the as-deposited thin films are partially crystalline with dense nanoparticles of $L2_1$ structure. The volume of crystalline particles increases during the course of sputtering and these particles are preferred growth on $(220)_A$ with particles' size being less than 50 nm. Experimental results also show that the

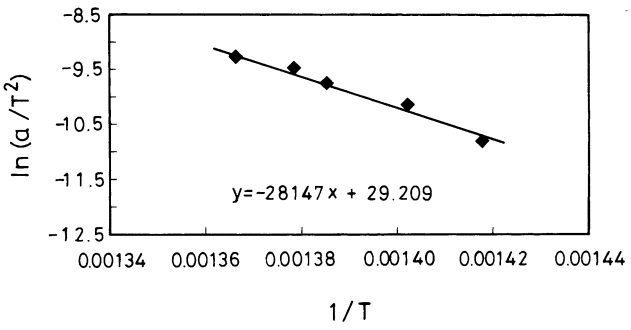


Fig. 5. Kissinger's plot for the DSC data of Fig. 4.

activation energy of crystallization, $Q$, of free-standing thin films is 234 kJ/mol by Kissinger's method. The onset crystallization temperature, $T_x$, is 427 °C at the 10 °C/min heating rate. Both of $Q$ and $T_x$ values of $Ni_{51.45}Mn_{25.30}Ga_{23.25}$ thin films are much lower than those of near equiatomic TiNi alloys. The characteristic of partially crystalline property inherent in the as-deposited $Ni_{51.45}Mn_{25.30}Ga_{23.25}$ thin films may account for the difference of crystallization behavior between TiNi and $Ni_2MnGa$ SMAs.

## Acknowledgments

The authors are grateful by the National Science Council (NSC), Republic of China, for financial support under the Grant NSC89-2216-E002-057.

## References

[1] V.V. Kokorin, V.A. Chernenko, Phys. Met. Metall. 68 (1989) 111.
[2] E. Cesari, V.A. Chernenko, V.V. Kokorin, J. Pons, C. Segui, Acta Mater. 45 (1997) 999.
[3] K. Ullakko, J.K. Huang, C. Kanter, R.C. O'Handley, V.V. Kokorin, Appl. Phys. Lett. 69 (1996) 1966.
[4] R.C. O'Handley, J. Appl. Phys. 83 (1998) 3263.
[5] R. Tickle, R.D. James, J. Magn. Magn. Mater. 195 (1999) 627.
[6] W.H. Wang, G.H. Wu, J.L. Chen, C.H. Yu, Z. Wang, Y.F. Zheng, L.C. Zhao, W.S. Zhan, J. Phys. Condens. Matter. 12 (2000) 6287.
[7] J.W. Dong, L.C. Chen, C.J. Palmstrom, R.D. James, S. McKernan, Appl. Phys. Lett. 75 (1999) 1443.
[8] M. Wuttig, C. Craciunescu, J. Li, Mater. Trans. JIM 41 (2000) 933.
[9] J.Z. Chen, S.K. Wu, Thin Solid Films 339 (1999) 194.
[10] H.E. Kissinger, Anal. Chem. 29 (1957) 1702.
[11] J.Z. Chen, S.K. Wu, J. Non-Cryst. Sol. 288 (2001) 159.